

BBA 74411

## Sensitive detection of protein adsorption to supported lipid bilayers by frequency-dependent capacitance measurements and microelectrophoresis

Martin Stelzle and Erich Sackmann

*Physik-Department (Biophysics Group), Technische Universität München, Garching-München (F.R.G.)*

(Received 9 December 1988)

**Key words:** Supported bilayer; Biosensor; Langmuir-Blodgett film; Protein adsorption; Lipid bilayer; Microelectrophoresis

In the first part, we report experiments which enable the sensitive detection of protein adsorption to lipid bilayers deposited onto chromium electrodes on glass substrates by frequency-dependent capacitance measurements. The sensitivity of the present type of sensor (better than 0.3 nm average protein layer thickness) is at least equivalent to that of ellipsometry. A high specific resistance of the supported bilayer of  $(1-5) \cdot 10^5 \Omega \cdot \text{cm}^2$  is achieved by deposition of a tightly packed (crystalline) cadmium arachidate monolayer in contact with the substrate, whereas the outer monolayer can be more loosely packed (fluid phase or state of fluid–solid coexistence) which is essential for the incorporation of receptors. In the present work, charged lipids are incorporated as nonspecific receptors for polylysine and cytochrome *c*. The capacitance measurements provide a very sensitive test of the tightness and the long-time stability of the supported bilayers and, in combination with ellipsometric thickness measurements, enable estimations of dielectric properties of protein layers (such as the permittivity). In the second part, we report first electrophoresis experiments in asymmetric bilayers on substrates which enable simultaneous measurements of lateral diffusion coefficients and frictional coefficients between monolayers. The potential application of the electrophoretic effect for the differentiation between different receptors and the amplification of signals in biosensors is discussed.

### Introduction

Some of the primary motivations for the growing interest in the coupling of lipid layers with solid surfaces are: (1) the preparation of biosensors [1,2], (2) applications in nonlinear optics [3] and (3) mimicking of biological processes of self-assembly and recognition processes [2,4,5]. The most pertinent problem to be solved for the first type of application is the preparation of stable high-resistance lipid/protein bilayers which at present is only possible in an aqueous environment [6].

In the present paper, we report on a sensor for the detection of adsorbed proteins on supported lipid bilayers which contain charged lipids as nonspecific receptors in the monolayer facing the aqueous phase. A

high specific resistance of the bilayers is already achieved if the monolayer in contact with the (chromium) electrodes is tightly packed, such as cadmium arachidate whereas the outer monolayer can be transferred from a fluid phase or a state of fluid–solid coexistence. The latter is essential for future incorporations of more specific receptors.

By measurement of the specific capacitance, the specific resistance and the electrolyte resistance in a frequency regime between 1 and 500 Hz, it is possible to detect adsorption layers of about 0.3 nm average thickness. This corresponds at least to the sensitivity of ellipsometry as is demonstrated in a separate experiment. In combination with thickness determinations by ellipsometry, the capacitance measurements can also yield information about the dielectric properties (e.g., the permittivity) of the protein layers. The present capacitance measurements also provide a sensitive tool for the detection of bilayer instabilities, in particular after protein adsorption.

In the second part, we report first microelectrophoresis experiments on supported bilayers which enable measurements of the frictional coefficients between the two opposing monolayers of a bilayer. The potential

Abbreviations: DPPC, dipalmitoylphosphatidylcholine; DMPC, dimyristoylphosphatidylcholine; DMPE, dimyristoylphosphatidylethanolamine; DMPA, dimyristoylphosphatidic acid; PS, phosphatidylserine; NBD-PG, dimyristoylphosphatidylglycerol (7-nitrobenz-2-oxa-1,3-diazol-4-yl)-labelled.

Correspondence: E. Sackmann, Physik-Department (Biophysics Group), Technische Universität München, D-8046 Garching-München, F.R.G.

application of this effect for (1) the separation of loaded and unloaded, (2) the separation of different receptors and (3) signal amplification is discussed.

### Preparation of sensor electrodes and capacitance measuring procedure

The sensor electrodes consist of glass plates ( $2.6 \times 7.6 \times 0.1 \text{ cm}^3$ ) onto which chromium layers ( $2.0 \times 1.0 \text{ cm}^2$ ) of variable thickness (20–50 nm) are vacuum deposited. Chromium is used as electrode material because it adheres much better on glass than, for instance, gold. Prior to the monolayer transfer, the electrode surface is made hydrophilic by argon sputtering in a microwave discharge.

Asymmetric lipid bilayers are deposited onto the freshly prepared substrates by the Langmuir-Blodgett-Kuhn technique following Tamm and McConnell [6]. In order to achieve a high specific resistance, the layer facing the electrode consists of tightly packed (that is crystalline) cadmium arachidate. It is deposited by pulling the substrates through an arachidonic acid monolayer kept at a lateral pressure of 30 mN/m, while the subphase contains  $10^{-3}$ – $10^{-4}$  M  $\text{CdCl}_2$  solution. The second layer consists of mixtures of zwitterionic (DPPC and DMPC) and charged lipid (either DMPA or brain PS).

The charged component serves as a nonspecific receptor for proteins [7]. The upper monolayer is deposited by transfer of the cadmium arachidate-covered substrate through the mixed monolayer into aqueous phase. Both the measuring and the counter electrode are prepared during the same working process and are covered by exactly the same bilayer. For the present capacitance measurements, it is convenient to leave the sensor electrodes in the aqueous phase during the experiment. They can, of course, also be transferred to a closed chamber for this measurement as is done in the case of the microelectrophoresis experiment.

The principle of the capacitance measurement is illustrated in Fig. 1. An a.c. voltage from a function generator (HP 8116A),  $U_0(f)$ , of constant amplitude and variable frequency is fed to the measuring electrode via resistor,  $R_0$ . In order to avoid electrochemical effects and membrane damage, the upper limit of  $U_0$  was 100 mV. The voltage,  $U_c(f)$ , at the measuring electrode is recorded by a (home-made) a.c. to d.c. converter.  $U_c(f)$  is determined by several parameters: (1) the specific capacitance,  $C_m$ , of the supported membrane and adsorption layer (in  $\mu\text{F}/\text{cm}^2$ ); (2) the corresponding value,  $C_g$ , of the diffuse Gouy-Chapman double layer at the membrane/water interface; (3) the specific resistance,  $R_m$ , of the supported bilayer (in  $\Omega \cdot \text{cm}^2$ ) and (4) the resistance  $R_2$  of the connecting lines ( $R_m \gg R_2$ ).

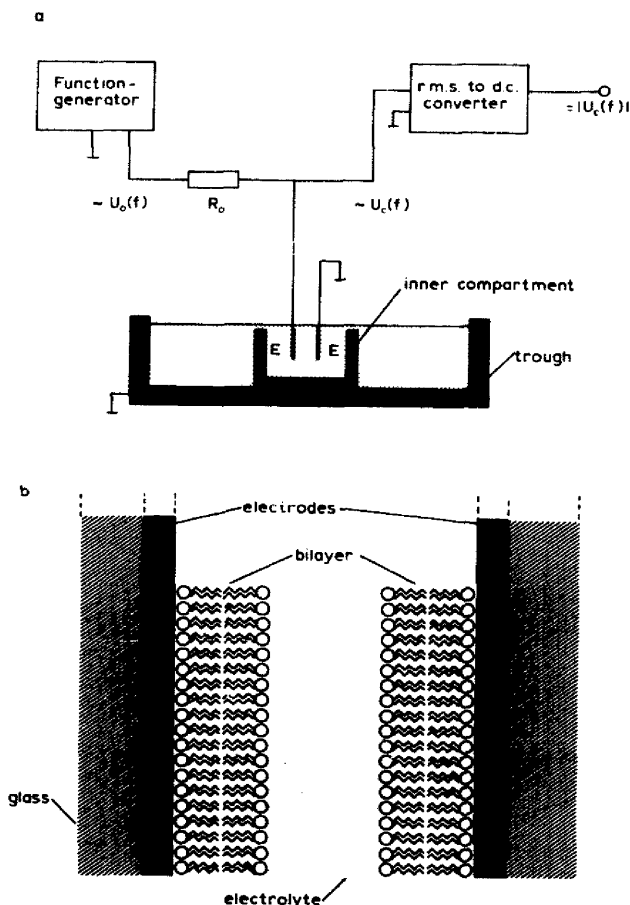


Fig. 1. Assembly for measurement of the frequency-dependent impedance of the sensor. An a.c. voltage with constant amplitude  $U_0$  from a function generator (HP 8116A) is applied to one of the (identically prepared) electrodes via the resistor  $R_0$ . The counter electrode is connected to ground. The measured voltage  $U_c(f)$  is fed to an home-made r.m.s. to d.c. converter and recorded. (b) Sensor electrodes consisting of glass substrates ( $2.6 \times 7.6 \times 0.1 \text{ cm}^3$ ) onto which chromium electrodes ( $1.0 \times 2.0 \text{ cm}^2$ ), are vacuum-deposited, while the whole surfaces of both electrodes are covered by a lipid bilayer which is deposited by the Langmuir-Blodgett-Kuhn technique. The electrodes remain in an inner compartment of 30 ml volume which is in the trough of the film balance during the present measurement.

A detailed equivalent circuit of the sensor is presented in Fig. 2. Each electrode is a parallel circuit of  $R_m$  and  $C_m$ . However, the membrane capacitance,  $C_m$ , itself, is a parallel connection of that of the bilayer  $C_{m0}$  and of that of the (Gouy-Chapman) layers at the defects or holes through the bilayer which is denoted as  $C_h$ . If the area fraction covered by holes is given by  $(1 - \theta)$  and that covered by tight bilayer by  $\theta$ , one obtains

$$C_h = (1 - \theta) \cdot C_g$$

and

$$C_m = \theta \cdot C_{m0} + C_h \quad (1)$$

For the determination of  $C_m$  from the measured voltage,  $U_c(f)$ , the unknown specific capacitance,  $C_g$ , of the Gouy-Chapman layer can be neglected to a good approximation for the following reason. Measurements with uncovered electrodes show that for the ionic strength of  $10^{-2}$  M KCl,  $C_g$  is about  $25\text{--}30 \mu\text{F}/\text{cm}^2$ , in agreement with the Gouy-Chapman theory which predicts  $C_g = 33 \mu\text{F}/\text{cm}^2$ . Since the Gouy-Chapman capacitance is larger by more than one order of magnitude than the expected value of  $C_m$ , it acts as a short circuit at high frequencies. Neglecting  $C_g$ , the measured voltage,  $U_c$ , is given by

$$U_c(f; R_0, R_m, C_m, R_2) = U_0 \sqrt{\frac{(R_m + R_2)^2 + \omega^2 \tau_m^2 R_2^2}{(R_0 + R_m + R_2)^2 + \omega^2 \tau_m^2 (R_0 + R_2)^2}} \quad (2)$$

with  $\tau_m = R_m C_m$ ;  $\omega = 2\pi f$ .

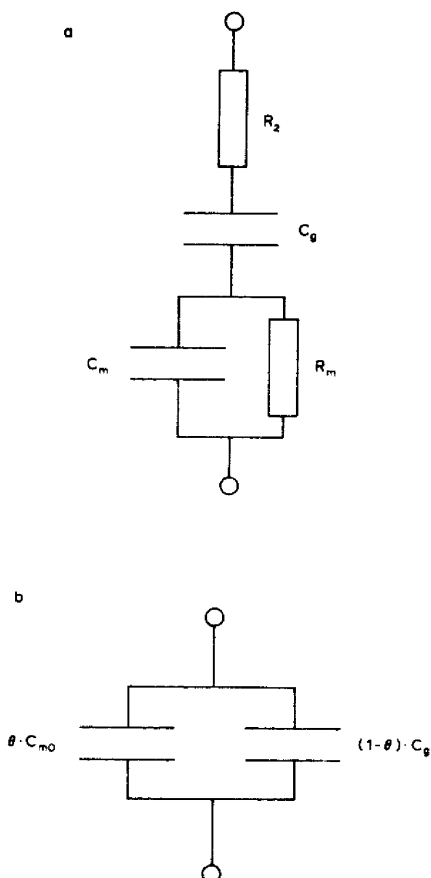


Fig. 2. (a) Equivalent circuit for determination of impedance of sensor in terms of the four pertinent parameters: the specific capacitances of the bilayer,  $C_m$ , and of the diffuse Gouy-Chapman layer  $C_g$  (in  $\mu\text{F} \cdot \text{cm}^{-2}$ ), the specific membrane resistance  $R_m$  (in  $\Omega \cdot \text{cm}^2$ ) and the resistance of the electrolyte and of connection lines  $R_2$ . (b) Superposition of specific membrane capacitance,  $C_m$ , from value of bilayer,  $C_{m0}$ , and of diffuse ion layer,  $C_g$ , at defects (holes) in bilayer;  $\theta$  is the area fraction covered by the tight bilayer.

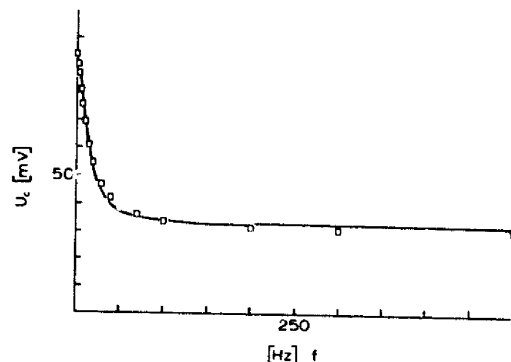


Fig. 3. Comparison of measured frequency-dependence of the pick-up voltage  $U_c(f)$  ( $\square$ ) with theoretical curve (—) calculated with the help of Eqn. 2. Both sensor electrodes are covered by the same cadmium arachidate-DPPC/DMPA bilayer where the former is in contact with the chromium electrode.

Fig. 3 shows that the above approximation is justified. The frequency-dependence of the measured voltage,  $U_c$ , is plotted for a sensor, the electrodes of which are covered by a cadmium arachidate-DPPC/DMPA bilayer, whereas the drawn curve is calculated from Eqn. 2. The deviation between the measured and the calculated curve is less than 2%.

Two measuring procedures are possible:

(1) Measurement of the impedance  $Z(f)$  (via measurement of  $U_c(f)$ ) of the system in the whole frequency range (1–500 Hz) followed by the determination of the parameters  $R_m$ ,  $C_m$  and  $R_2$  from  $U_c(f)$  (Eqn. 2).

(2) Continuous measurement of  $U_c(f_0; t)$  at a fixed frequency,  $f_0$ , at which  $U_c(f_0; t)$  is most sensitively dependent on the parameter of interest, which in our case is  $C_m$ . The value of  $f_0$  is obtained from  $\partial^2 U_c(f) / (\partial C_m \partial f) = 0$  and depends on  $R_m$ ,  $C_m$  and  $R_2$ . For the present measuring system, the sensitivity maximum ranges from 15 to 20 Hz.

In the present work the second method was adopted for simultaneous measurements of changes in  $C_m$  during the deposition of proteins.

## Results of capacitance measurements

### Multilayers of cadmium arachidate

In order to test the reliability of the capacitance measurement of lipid-covered electrodes immersed in water, the specific resistance,  $R_m(n)$ , and specific capacitance,  $C_m(n)$ , of a multilayer of cadmium arachidate is measured. The multilayer is transferred at 32 mN/m in the presence of  $2.5 \cdot 10^{-4}$  M  $\text{CdCl}_2$  in the subphase. In the case of a series connection of  $n$  identical monolayers with specific capacitance,  $C_0$ , and specific resistance,  $R_0$ , one would expect  $C_m(n) = C_0/n$  for the total specific capacitance of the multilayer and  $R_m(n) = R_0 \cdot n$  for its total specific resistance. The experimental result is shown in Fig. 4. Above  $n = 2$ , the

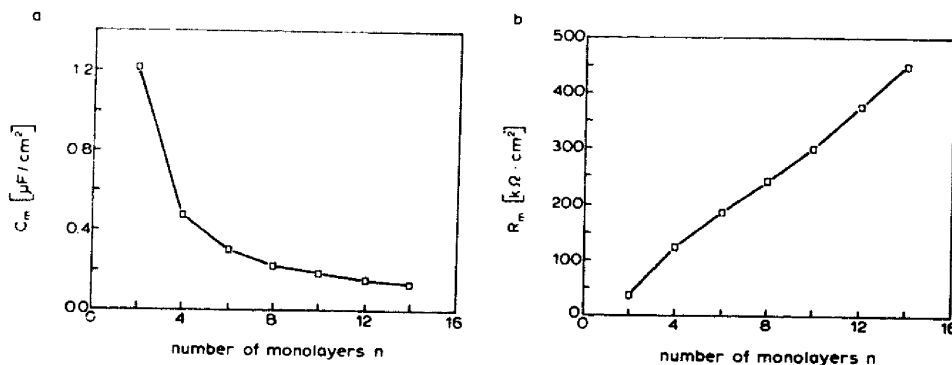


Fig. 4. Plot of specific capacitance,  $C_m(n)$ , (Fig. 4a) and specific resistance,  $R_m(n)$ , (Fig. 4b) of multilayers of cadmium arachidate as a function of the number  $n$  of monolayers. The sensor electrodes are kept immersed in the aqueous phase during the whole measurement. After each measurement with  $n$  monolayers, the electrodes are pulled out of and pushed into the trough again, in order to deposit the subsequent bilayer.

specific capacitance,  $C_m$ , decreases like  $1/n$  and the specific resistance increases linearly with increasing number of monolayers  $n$ :

$$C_m(n) = (1.8 \mu\text{F}/\text{cm}^2)/n$$

$$R_m(n) = (-22 + 33.3 \cdot n) \text{ k}\Omega \cdot \text{cm}^2$$

For the first two layers, however,  $C_m(n)$  is larger and  $R_m(n)$  smaller than expected from the above relationships. This is clearly a consequence of the defects in the bilayer in direct contact with the electrodes. Assuming that at  $n > 4$  the bilayers are defect-free, the area fraction  $(1 - \theta)$  covered by defects can be estimated to 2.1%.

#### Detection of polylysine adsorption

As a good example of the influence of protein adsorption on the sensor capacitance, we show the effect of the addition of polylysine to the subphase on the specific capacitance of electrodes covered by cadmium arachidate as inner and a 1:1 mixture of DPPC and

DMPA (as receptor) as outer monolayer. The sensor voltage  $U_c(f_0 = 10 \text{ Hz}; t)$  and the membrane capacitance,  $C_m$ , as obtained from Eqn. 2 are shown in Fig. 5. The record is started about 5 min after transfer of the outer monolayer. After deposition of the bilayer, the voltage decreases slowly with time owing to a small instability of the bilayer. Injection of polylysine to the subphase clearly leads to a remarkable increase in the voltage and a corresponding decrease of the membrane capacitance,  $C_m$ . The polylysine ( $M_r$  30 000–70 000) has been added in three steps (each time  $60 \mu\text{g} = 10^{-9} \text{ mol}$ ) to the inner compartment of 30 ml volume. It is seen that saturation is, in fact, reached already after the second step. The total increase in  $U_c$  is 3% and the decrease in the membrane capacitance is about 5%. The fact that  $C_m$  decreases shows that the thickness of the bilayer is really increased owing to the adsorption of the polymer. According to Fig. 5, the voltage,  $U_c$ , exhibits long time stability after the protein addition, which shows that the DPPC/DMPA monolayer is stable also after the adsorption process.

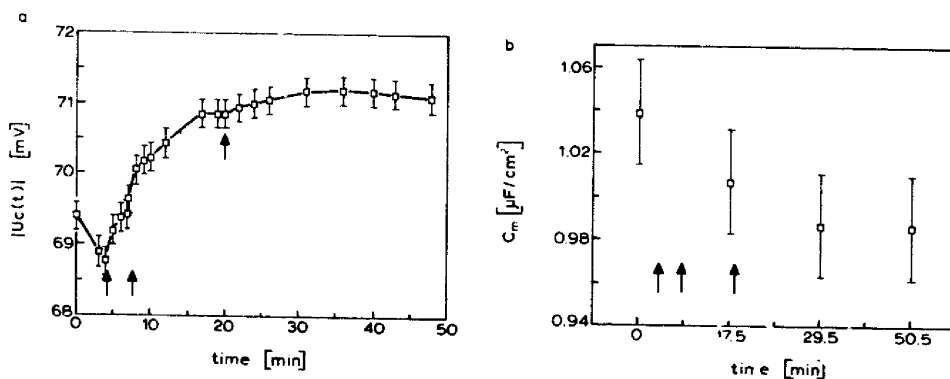


Fig. 5. (a) Time-dependence of measured voltage  $U_c$  of sensors covered by cadmium arachidate as inner and a 1:1 DPPC/DMPA mixture as outer monolayer prior to and after addition of polylysine ( $M_r$  30 000–70 000). At the times indicated by arrows,  $60 \mu\text{g}$  of polylysine are injected between the electrodes into the inner 30 ml compartment (which corresponds to about  $10^{-9} \text{ mol}$ ). The measuring frequency is 10 Hz. The vertical bars indicate the accuracy of the voltage measurement ( $\pm 0.2 \text{ mV}$ ). (b) Variation of membrane capacitance,  $C_m$ , with time as obtained from frequency scans of  $U_c$  and evaluation with Eqn. 2.

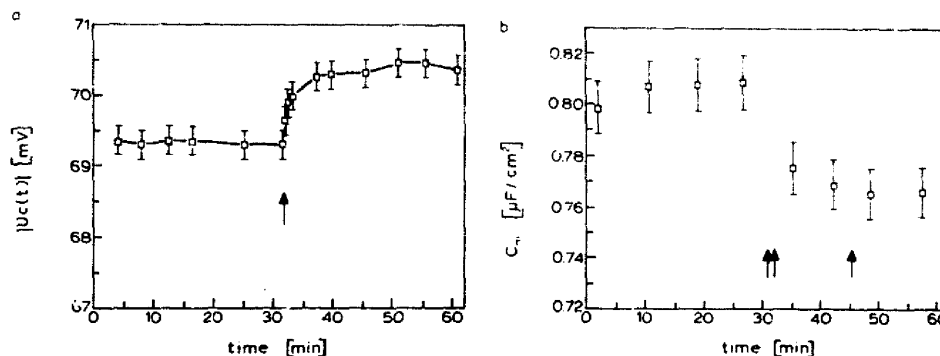


Fig. 6. (a) Time-dependence of voltage,  $U_c(t)$ , and its variation caused by addition of cytochrome *c* of sensor with 1:1 mixture of DPPC and DMPA as outer monolayer. About 80  $\mu g$  of the protein are added to the 30 ml of subphase which corresponds to  $6.5 \cdot 10^{-9}$  mol ( $M_r$  of cytochrome *c* = 12400). Measuring frequency is 15 Hz. The vertical bars indicate the accuracy of the voltage measurement ( $\pm 0.2$  mV). (b) Effect of cytochrome *c* adsorption on specific capacitance  $C_m(t)$ .

In contrast, sensors with DMPC/PS mixed monolayers at the outside are much less stable already before the addition of polylysine to the subphase. In this case, the specific membrane capacitance increases with time (by 3% per min) after polymer addition. This can be explained in terms of the forming of holes and/or the removal of unsaturated brain PS by the protein

#### Detection of cytochrome C adsorption

An example of more biological relevance is shown in Fig. 6. The sensor electrodes are covered by a 1:1 mixture of DPPC and DMPA at the outside. First, it is seen that both the voltage  $U_c(f_0 = 15 \text{ Hz}; t)$  and the membrane capacitance  $C_m$  are constant over some 30 min, showing that the supported bilayer which is transferred at  $t = 0$  is stable. Aliquots of 80  $\mu g$  of cytochrome *C* are added to the inner compartment of 30 ml volume (corresponding to  $6.5 \cdot 10^{-9}$  mol) at the times indicated by arrows in Fig. 6b. The voltage increases by 1.2 mV (or 1.7%) and the specific capacitance decreases by 40 nF/cm<sup>2</sup> after addition of two aliquots after which saturation is already observed.

#### Discussion of adsorption studies

Fig. 5 and 6 demonstrate that sensor electrodes with supported bilayers exhibit a rather high long-time stability if the monolayer in contact with the chromium electrode is tightly packed. From the complete analysis of the sensor impedance according to Eqn. 2, it follows that the specific electric resistance of the electrodes varies between 100 and 500  $k\Omega \cdot cm^2$ , which is quite high but still three orders of magnitude smaller than the characteristic value of black membranes [7].

If one assumes that the adsorbed protein layer can be considered as a homogeneous dielectric film of thickness  $d_a$  and dielectric constant  $\epsilon_a$  and that the conductivity of the bilayer is negligibly small, its specific capacitance,  $C_a$ , is:

$$C_a = \epsilon_0 \epsilon_a / d_a$$

It is in series connection with the specific capacitance,  $C_m$ ,

$$C_m = \epsilon_0 \epsilon_m / d_m$$

of the pure lipid bilayer. It is easily verified that the change in the total (specific) membrane capacitance owing to the protein adsorption is

$$\frac{\Delta C_m}{C_m} = - \frac{\epsilon_m (d_a / d_m)}{\epsilon_a + \epsilon_m (d_a / d_m)} \quad (3)$$

This equation shows firstly that the supported lipid bilayer must be very thin in order to reach a high sensitivity, which is the case for supported single bilayers. Secondly, the thickness of the adsorbed layer can be estimated if the dielectric constant of the protein layer is known or vice versa. The dielectric constant may be determined if the adsorbed layer thickness is determined in a separate experiment. The latter procedure has been applied in the case of polylysine.

The thickness of the adsorbed polylysine layer on the bilayer composed of cadmium arachidate and a 1:1

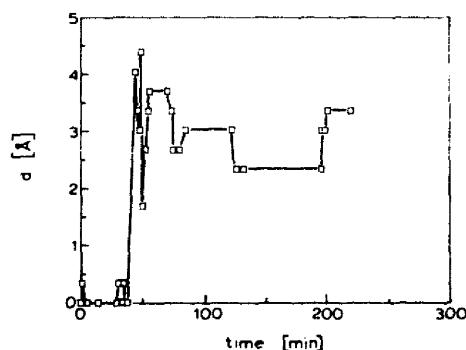


Fig. 7. Ellipsometric measurement of change of thickness of supported bilayer consisting of cadmium arachidate as inner and a 1:1 mixture of DPPC and DMPA as outer monolayer. At  $t = 33.5$  min,  $2 \cdot 10^{-9}$  mol of polylysine have been added to the subphase (vol. 6.6 ml). According to Fig. 5, this corresponds to saturation.

DPPC/DMPA mixture has been determined by ellipsometry. The result is shown in Fig. 7; the thickness changed by 0.3 nm after addition of 100  $\mu\text{g}$  of the polypeptide to 6.6 ml of the buffer. From the difference in the values of  $C_m$  (measured with other, but identically prepared electrodes) prior to ( $1.039 \pm 0.024 \mu\text{F}/\text{cm}^2$ ) and after ( $0.986 \pm 0.024 \mu\text{F}/\text{cm}^2$ ) addition of the polylysine until saturation is reached (see Fig. 5), one obtains from Eqn. 3  $C_a = 19.3 \mu\text{F}/\text{cm}^2$ . This yields a ratio of  $d_a/\epsilon_a = 0.08 \pm 0.05 \text{ nm}$ . The large error is due to the fact that two large numbers have to be subtracted for the determination of this ratio. Comparison of the capacitance and the ellipsometric measurement yields a dielectric constant for polylysine of  $\epsilon_a = 3.8$ .

Consider now the case of cytochrome *c* adsorption. From the observed change in capacitance at saturation, one obtains in the same way as in the case of polylysine  $C_a = 14.2 \pm 4.7 \mu\text{F}/\text{cm}^2$ . This yields a ratio of  $d_a/\epsilon_a = 0.07 \pm 0.02 \text{ nm}$ .

### Microelectrophoresis in supported bilayers

Two essential problems of biosensor research are the discrimination between different receptors and signal amplification. One conceivable solution to these problems could be based on the lateral reorganization of receptors by electrophoresis after the binding process. As shown below, the present technique of asymmetric bilayer deposition allows such a reorganization. For that experiment, two chromium electrodes which are separated by a small gap of 80  $\mu\text{m}$  are vacuum-deposited onto a microscope coverglass as shown in Fig. 8a. After the deposition of the bilayer, the coverglass is put onto a microslide with a waterfilled mould in the center in such a way that the bilayer is in contact with the water (Fig. 8b). This is performed under water and after removal the gap between the two glass plates is sealed with nail varnish.

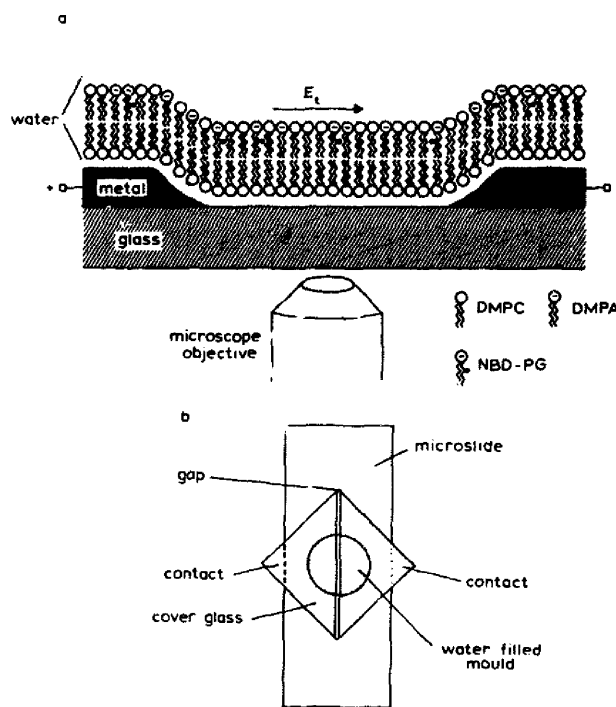


Fig. 8. (a) Schematic view of a microelectrophoresis experiment, showing the electrode with the supported bilayer. The latter consists of a DMPC monolayer adjacent to the substrate and a 3:1 mixed monolayer of DMPC and DMPA to which 2 mol% of NBD-PG is added. (b) Electrode consisting of microscope cover glass ( $2.4 \times 2.4 \text{ cm}^2$ ) with two vacuum-deposited chromium electrodes which are separated by a 80  $\mu\text{m}$  wide gap stretching along one diagonal. This glass plate is deposited onto a microslide with a water-filled groove in such a way that the bilayer is in contact with water. The plates are sealed at the rims by nail varnish.

For the experiments in the present work, the bilayer consists of DMPC as inner and a 3:1 DMPC/DMPA mixture (doped with 2 mol% NBD-PG) as outer monolayer. The former is deposited from 10 mN/m and is thus in the fluid state and the latter from 15 mN/m and is thus in a state of fluid-solid coexistence [8].

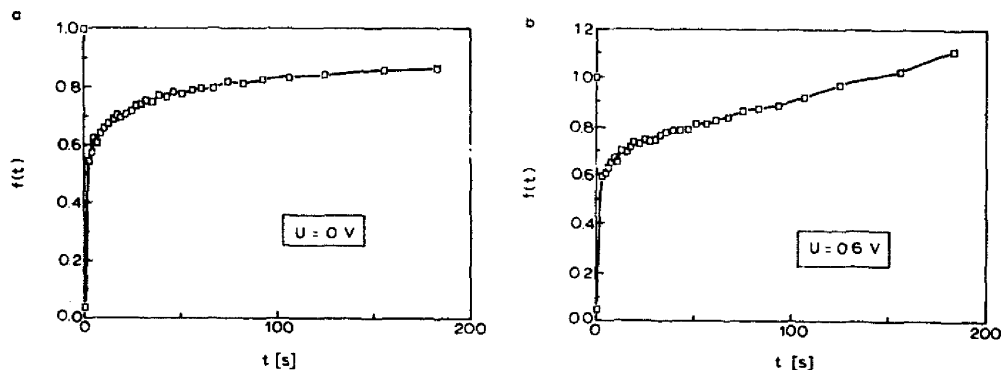


Fig. 9. Fluorescence-recovery curve observed without (Fig. 9a) and with (Fig. 9b) application of a d.c. voltage. The ratio  $f(t) = F(t)/F(0)$  of the fluorescence intensity at time  $t$  divided by the intensity at time zero (that is, prior to bleaching) is plotted as a function of time. Note the characteristic difference in the long-time behaviour.

The electrophoretic effect is studied by the familiar fluorescence recovery after photobleaching (FRAP) technique [9]. The fluorescence label is bleached within a circular patch of radius  $w = 15 \mu\text{m}$  by imaging an argon laser beam onto the bilayer via the microscope objective (see Fig. 8a) through which the recovery of the fluorescence is also observed.

Fig. 9 shows two typical fluorescence-recovery curves as obtained in the absence or presence of a electric d.c. voltage of 0.6 V. The ordinate gives the ratio,  $f(t)$ , of the fluorescence intensities  $F(t)$  measured at time  $t$  after bleaching to the intensity  $F(0)$  before bleaching (time  $t = 0$ ). The two curves differ clearly, in particular in the long-time behaviour. In the absence of the d.c. field,  $f(t)$  exhibits a behaviour typical for recovery of the fluorescence by lateral diffusion of unbleached dye molecules into the bleaching spot. In the presence of the field, one observes two regimes: at short times,  $f(t)$  is similar to the diffusion-controlled process, whereas, at long times,  $f(t)$  increases linearly with time. As is well-known, the latter is typical for lipid flow [9], demonstrating the feasibility of electrophoresis within supported bilayers.

In the case of the absence of the field, the coefficient of lateral diffusion,  $D$ , is obtained from the time,  $T_{1/2}$ , after which half of the final fluorescence recovery is reached according to Ref. 9:

$$D = 0.22 \frac{w^2}{T_{1/2}}$$

where  $w$  is the radius of the bleaching spot. In the presence of the electric field, the recovery is determined also by the drift of the fluorescent probe characterized by the drift velocity

$$v = \frac{D}{k_B T} qE$$

where  $q$  is the charge of the probe and  $E$  the electric field strength. An approximate evaluation of the recovery curve in terms of the diffusion coefficient,  $D$ , and the drift velocity,  $v$ , is possible for rectangular bleaching profiles, a situation which is realized in the present experiment.

As shown in more detail in the Appendix, the initial regime of the recovery curve is determined by the random motion and the long-time regime by the drift motion.

The above approximate evaluation procedure yields a value of  $D = 2.5 \cdot 10^{-8} \text{ cm}^2/\text{s}$ , which is in good agreement with other lateral diffusion measurements from this laboratory. For the drift velocity we obtain for 0.6 V a value of  $v = 0.18 \pm 0.02 \mu\text{m/s}$ . The fluorescent dye carries one negative charge and from the measured value of  $D$  one would thus expect a drift velocity of

$v = 0.75 \mu\text{m/s}$  if the whole voltage decrease across the two electrodes was effective. The discrepancy is explained in terms of a partial shielding of the electric field by accumulation of counterions at the bilayer/water interface. In fact, the current decays from 5 to 1  $\mu\text{A}$  in the course of time during an experiment. This behaviour is attributed to the capacitance,  $C_g$ , of the Gouy-Chapman layer on the electrodes.

## General discussion and conclusions

The present work demonstrates that it is possible to deposit asymmetric bilayers on electrode-covered substrates which exhibit both a high specific resistance and a low specific capacitance. Both are necessary conditions for the design of high-sensitivity sensors. We find that in order to achieve a high specific resistance only the monolayer in contact with the electrode must be tightly packed, while the outer monolayer can be deposited from the fluid-solid coexistence, that is, a low density state. The latter is essential for the incorporation of amphiphilic receptors other than charged lipids (such as lipid-coupled Fab fragments of antibodies or monopolar receptors). The specific resistance of the supported bilayers is still about three orders of magnitude smaller than that of black lipid membrane [7]. However, it will probably increase if the surface roughness of the electrodes is reduced.

The sensitivity of the measurement of changes in membrane capacitance,  $C_m$ , depends on the frequency. For the present design, the highest sensitivity is observed at about 15 Hz. For the present experiments, the electrodes are kept in the subphase of the trough during the whole measurement. However, it is easily possible to transfer the sensor electrodes to a cuvette below water, as is done for instance for the electrophoresis experiment. The present capacitance measurements can also be applied to test the quality (such as the tightness) and the long-time stability of supported bilayers in a much more sensitive way than is possible for instance by lateral diffusion or microfluorescence experiments. Since the formation of holes in the bilayer leads to a strong increase in the membrane capacitance (owing to  $C_g$ ), whereas pure adsorption decreases  $C_m$ , instabilities of the supported bilayer caused by the interaction with the proteins can be sensitively detected. Last but not least, capacitance measurements in combination with ellipsometry can yield information about electric properties (such as permittivities) of protein layers or dipole moments of proteins.

Two major problems of the sensor design are the amplification of the signals and the differentiation between loaded and unloaded receptors of the same type or between different receptors. One possible solution to both problems is the lateral reorganization of the receptors after the binding process. Such a reorganization is

possible by microelectrophoresis if the outer monolayer is transferred from a fluid state. The electrophoretic effect is, of course, much smaller than that achieved in monolayers at the air/water interface [10]. The electrophoresis is also of more general interest. It can be exploited in order to measure the friction between two opposing monolayers of a bilayer and to estimate the change of adsorbed ligands.

## Appendix

### Evaluation of drift velocity

The recovery of the fluorescence owing to the flow of the fluorescent probe in the electric field is obtained from the drift velocity,  $v$ , of the bleaching spot as indicated in Fig. 10. For rectangular bleaching profiles, the observed fluorescence intensity is proportional to the ratio of the area  $A$  (Fig. 10) to the total area  $\pi w^2$  of the bleached spot. If  $B$  is the degree of bleaching (relative reduction in intensity), the ratio of the fluorescence intensity at time  $t$ ,  $F(t)$ , to that at time  $t=0$  prior to bleaching,  $F(0)$ , is

$$f(t) = \frac{F(t)}{F(0)} = 1 - \frac{2B}{\pi} (\arccos(x) - x\sqrt{1-x^2})$$

$$\text{with } x = \cos \phi = \frac{vt}{2w}$$

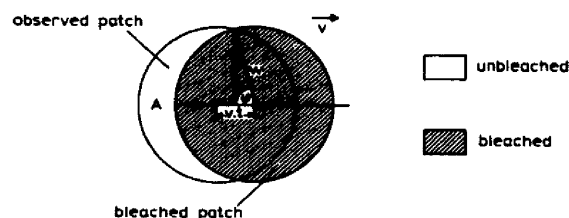


Fig. 10. The calculation of the fluorescence recovery by lipid flow in the electric field in the case of a rectangular bleaching profile.

The range of migration in the time interval  $T$  is  $\sqrt{DT}$  in the case of diffusion and  $vT$  in the case of flow. Therefore, the initial region of the recovery curve is determined by diffusion and the final stage by the flow. As has been shown by model calculations, it is indeed possible to determine  $D$  by evaluation of measurements without flow (electric field  $E=0$ ) and  $v$  of the later part of the observed recovery curves with flow ( $E \neq 0$ ).

## Acknowledgements

The present work was supported by the Fonds der Chemischen Industrie and by the Freunde der Technischen Universität München. Helpful discussions with H. Gaub and his laboratory are gratefully acknowledged.

## References

- 1 Turner, A.P.F., Karube, I. and Wilson, G.S. (1987) *Biosensors Fundamentals and Applications*, Oxford University Press.
- 2 Rubinstein, I., Steinberg, S., Tor, Y., Shanzer, A. and Sagiv, J. (1988) *Nature* 332, 426–429.
- 3 Swalen, J.D., Allara, D.L., Andrade, J.D., Chandross, E.A., Garoff, S., Israelachvili, J., McCarthy, T.J., Murray, R., Pease, R.F., Rabolt, J.F., Wynne, K.J. and Yu, H. (1987) *Langmuir* 3, 932.
- 4 Sackmann, E., Eggl, P., Fahn, C., Bader, H., Ringsdorf, H. and Schollmeier, M. (1985) *Ber. Bunsenges. Phys. Chem.* 89, 1198–1208.
- 5 Kuhn, H., Möbius, D. and Bücher, H. (1972) in *Physical Methods of Chemistry* (Weissberger, A. and Rossiter, B.W., eds.), Vol. 1, pp. III B57, Wiley, New York.
- 6 Tamm, L.K. and McConnell, H.M. (1985) *Biophys. J.* 47, 105–113.
- 7 Läuger, P. (1985) *Angew. Chem. Int. Edn.* 24, 905–920.
- 8 Fischer, A. and Sackmann, E. (1985) *J. Colloid Interface Sci.* 112, 1–14.
- 9 Axelrod, D., Koppel, D.E., Schlessinger, J., Elson, E. and Webb, W.W. (1976) *Biophys. J.* 16, 1055–1068.
- 10 Miller, A. and Möhwald, H. (1986) *Europhys. Lett.* 2, 67–71.